2021 IEEE International Conference on Autonomous Systems (ICAS) | 978-1-7281-7289-7/21/$31.00 ©2021 IEEE | DOI: 10.1109/ICAS49788.2021.9551189

AUTOMATED PARKING TEST USING ISAR IMAGES FROM AUTOMOTIVE RADAR

Neeraj Pandey, Shobha Sundar Ram

Indraprastha Institute of Information Technology Delhi, New Delhi 110020 India
E-mail: {neerajp, shobha}@iiitd.ac.in

ABSTRACT

Automated driving tests using cameras have been researched for expediting the training and testing of car drivers. We propose an automated parking test using millimeter-wave automotive radars. The advantage is that these radars can be operated even in low visibility conditions. We propose generating high-resolution inverse synthetic aperture radar (ISAR) images of a vehicle under test (VUT) parking into a designated parking slot from an externally mounted radar. The trajectory of the motion is estimated from the ISAR data using polynomial curve fitting from which the VUT is deemed to have either correctly or incorrectly parked. We experimentally validate the proposed method with millimeter-wave radar data gathered for cars performing perpendicular and 45° angle parking.

Index Terms— ISAR, Parking test, Automotive radar

1. INTRODUCTION

A key component towards improving road safety is to have well-trained and tested automobile drivers on the road. Recently, there has been research and development of automated driving license tests in order to address the costs, man-hours and other types of inadequacies associated with manual driving tests such as the tedium and corruption of the driving test inspectors. Driving tests typically involve testing the drivers in several key components such as lane changing, turning, following road rules, and parking. Currently, cameras have been the sensors of choice for automotive license tests [1]. In this paper, we propose the use of millimeter-wave radars specifically for conducting automated parking tests. The main advantage of radar over other sensors such as cameras is that they can be used in low light/visibility conditions. Frequency modulated continuous wave radars are currently heavily used in automotive systems for pedestrian detection, blind spot detecting, object classification, and collision avoidance [2]. In our work, we propose that we use high-resolution radar images to test if the driver is following the designated test trajectory to the final parking spot.

Concurrent to automatic license testing development are the parking assistance systems on automobiles using cameras, lidars, and radars. These systems have been used to detect occupancy of parking slots [3, 4] and in aiding the drivers in the correct positioning of the vehicle, especially while backing in [5]. The main distinction between the system that we propose to the existing parking assistance systems is that the radar is mounted *outside* the vehicle. Thus the objective is to *test/train* the driver as opposed to *assisting* the driver to complete the parking. Second, conventional automotive radars provide point cloud information of the target scatterers in the radar field-of-view. Each scatterer is marked with associated features of range, Doppler velocity, and signal strength. High-end systems consisting of multiple receiver channels provide additional azimuth and elevation information as well. In the proposed system, instead of generating point cloud data of the scatterers on the vehicle, we consider a low cost and complexity, single-channel wideband radar, and generates high-resolution range-crossrange images using inverse synthetic aperture radar (ISAR) imaging techniques.

ISAR imaging is an established technique for generating high-resolution radar images of turning targets using single-channel radar data and has been extensively researched for airborne, waterborne, and ground-based vehicles [6]. ISAR, essentially, exploits the turning motion of a target to synthesize a large cross-range aperture in order to obtain fine cross-range resolution. In the past few years, there have been significant studies of both synthetic aperture radar (SAR) [7], and ISAR imaging of automotive targets using wideband data [8, 9, 10] for target detection and classification. These works have shown that these types of radar images provide rich information of the size, orientation, and trajectory of dynamic targets [10, 11]. The main challenges of ISAR are twofold: First, the translational motion parameters of the automotive targets must be properly estimated in order to calibrate/compensate for their translational motion; second, the angular turning velocity must be accurately measured in order to obtain accurate cross-range estimates. In the parking test that we propose, we specifically address these challenges by determining if the parking is correct based on the estimated two-dimensional trajectory followed by the vehicle under test (VUT) using the ISAR images. We have experimentally validated our proposed parking test using measurement radar data gathered from the 77 GHz Texas Instruments AWR-1843 automotive radar. Wide-band single channel radar data gathered along the target trajectory are suitably processed to obtain ISAR images from which the trajectory of the target is estimated.

We can summarize our main contributions in this paper as follows- First, we have proposed using ISAR images generated from a single channel externally mounted automotive radar for two types of parking - angle parking and perpendicular parking; Second, we have developed an automated parking test algorithm that uses these ISAR images to test if the parking maneuver is correct. Our paper is organized as follows. In the following section, we present the theory of radar signal, signal processing, and the parking test algorithm. In Section.3, we present the details of the experimental set up followed by the results in Section 4. Finally, we conclude the paper in Section 5.

2. THEORY

Radar Signal: We assume that the VUT is moving on the XY ground plane with the height along the Z axis. The automotive radar is mounted outside of the car in a fixed position at the origin. The radar is operated from a short-range from the VUT in a line-of-sight environment. The radar transmits a frequency modulated continuous wave radar signal as given by

$$S_{tx}(\tau) = rect\left(\frac{\tau}{T_{PRI}}\right) e^{j2\pi f_c \tau} e^{j\pi K \tau^2}, \quad (1)$$

where f_c is the carrier frequency, and the K is the chirp rate of the transmitted signal. In (1), $rect\,(\cdot)$ indicates that the transmitting signal is defined for the pulse repetition interval T_{PRI}. At short ranges, we consider the VUT as an extended target with B point scatterers. We assume that the amplitude of each point scatterer, a_b, slowly fluctuates and hence is constant within a coherent processing interval (T_{CPI}). Each point scatterer is dynamic, and the time-varying range of the scatterer is $r_b(t) = R_b + v_b t$, where R_b is the starting distance from the radar and v_b is the relative radial velocity with respect to radar. Here, t is the slow time across multiple pulses comprising one T_{CPI}. Due to the motion of the scatterer, the backscattered radar signal is Doppler shifted by $f_{D_b} = \frac{2v_b f_c}{c}$, where c is the velocity of light. The down-converted radar received signal from the target can be expressed in terms of fast (τ) and slow time as

$$S_{rx}(\tau, t) = \sum_{b}^{B} a_b(t) rect\left(\frac{\tau - \frac{2r_b}{c}}{T_{PRI}}\right) e^{j2\pi f_c \frac{2r_b(t)}{c}} e^{j\pi K(\tau - \frac{2r_b(t)}{c})^2} + \mu, \quad (2)$$

where μ is the additive receiver noise. The radar signal is sampled at sampling frequency f_s resulting in N fast time samples in every PRI and M slow time samples in every T_{CPI}. Thus, the discrete form of (2) is given by

$$S_{rx}[n, m] = \sum_{b}^{B} a_b[m] rect\left[\frac{n - n_b}{N}\right] e^{-j\frac{4\pi f_c}{c} R_b} e^{-j2\pi m f_{D_b} T_{PRI}} e^{j\pi K \frac{1}{f_s{}^2}(n - n_b)^2} + \mu, \quad (3)$$

where n_b is integer rounded from $\frac{2r_b(t)}{cf_s}$. The Doppler shift in (3) is due to both the translational as well as rotation motion of the target. Our first step in processing the digitized radar data is to perform translational motion compensation within each T_{CPI} based on [12, 6]. In the interests of space, we are not discussing these steps in complete detail. The range compensated signal is processed using the two-dimensional (2D) Fourier transform along the fast and slow time dimensions to obtain the range-Doppler ambiguity plot, as shown in

$$\chi[r, f_d] = 2DFT\{S_{rx}[n, m]\}. \quad (4)$$

We map the Doppler axis in the ambiguity plot to the crossrange - axis using an estimate of the angular velocity ω of the target for the corresponding T_{CPI} as shown in

$$\chi[r, f_d] \overset{f_d \times \frac{\lambda_c}{2\omega}}{\rightarrow} \chi[r, cr]. \quad (5)$$

The assumption is that the angular velocity is constant during the T_{CPI}. The Doppler axis f_d is multiplied by $\frac{\lambda_c}{2\omega}$ where λ_c is the wavelength corresponding to f_c in free space. There are many ways to estimate the angular velocity, ω, of a cooperative target such as the use of additional sensors such as gyrometers and accelerometers. In this work, we estimate the ω for every T_{CPI} from the change in the yaw, θ, over consecutive intervals, where $\theta[m]$ is

$$\theta[m] = \arctan\left(\frac{y_C[m] - y_C[m-1]}{x_C[m] - x_C[m-1]}\right). \quad (6)$$

Here (x_C, y_C) are the coordinates of the centroid of the VUT chassis with respect to the radar. We compute these coordinates based on the initial location of the VUT, the predefined trajectory, and the duration that the VUT takes to complete the trajectory.

Parking Test Algorithm: In the parking test, we infer whether the VUT has been appropriately parked based on the estimated trajectory of the VUT. In the *training algorithm*, we perform the following steps: First, we collect L ISAR images of the car following a correct trajectory into the designated parking slot. Then we collect a similar set of ISAR images of the car following several incorrect trajectories resulting in parking outside of the designated parking slot. Then for each trajectory (both correct and incorrect), we convert the images to gray-scale. Then we choose a 2D bounding box comparable to the length and width of the car and slide the center of the box across the pixels of each l^{th} image while keeping the dimensions of the box fixed. For each sliding position of the bounding box, we compute the sum of the energy in the corresponding pixels bounded by the box.Then, we identify the 2D pixel position, x_c^l, y_c^l which has the maximum energy as the dominant scattering center position for that l^{th} image. We repeat these steps across all L ISAR images corresponding to the VUT motion. Then we curve fit a 2D polynomial across the dominant scatterer position to estimate the trajectory of the VUT across all the L images. We hypothesize that this two-dimensional polynomial function will correspond approximately to the trajectory of the center of the car. We repeat the exercise for the motion of the car along the incorrect trajectories. These polynomial functions are stored and used while testing.

During the *test*, similar polynomials are estimated for the VUT motion and compared to the polynomials generated from the training. Then the VUT parking motion is deemed to be either correct or incorrect based on the closest fit of the test polynomial to the training polynomials. The advantages of this simple parking test are that the speed of VUT need not be identical to those of the car used for training. Hence, auxiliary sensors for estimating the translational motion characteristics of the test vehicles are not required. Further, the size of the VUT can differ a little from that used during training by adjusting the size of the bounding box.

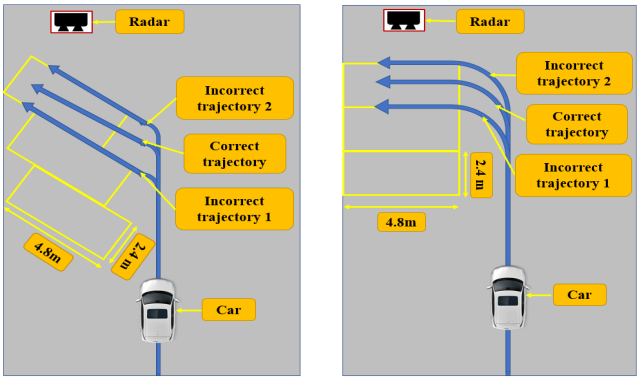

(a) (b)

Fig. 1. Three trajectories for the parking test for (a) 45° angle parking and (b) perpendicular parking.

3. EXPERIMENTAL SET UP

We use the Texas Instruments AWR 1843, a 77GHz millimeter-wave radar, for experimental data collection. We configure the radar to transmit a frequency modulated continuous wave signal with the parameters listed in Table 1 to operate as a short-range radar.The transmitted radar signal's pulse repetition interval (T_{PRI}) is set to be 400

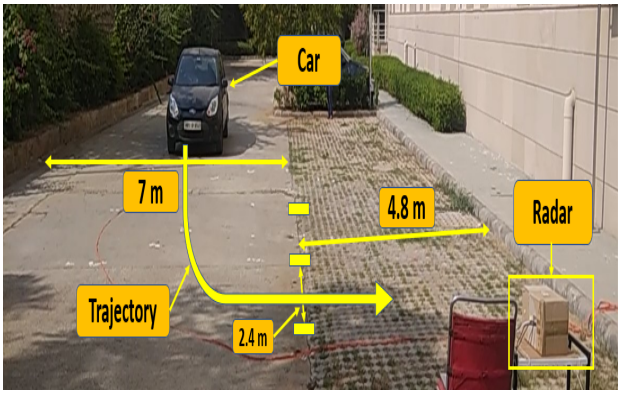

Fig. 2. The experiment setup for the parking test radar is situated at the location (0,0,0.5)m, and the car is parking at perpendicular parking.

Table 1. Automotive radar TI-AWR 1843 parameters for generating ISAR images

Parameters	Values
Carrier frequency (f_c)	77GHz
Sampling Frequency (f_s)	5MHz
Bandwidth (BW)	2GHz
Chirp rate (K)	7.5×10^{12} Hz^2
Chirp duration (T_{PRI})	400μs
Coherent processing interval (T_{CPI})	0.1s
Ramp time	267 μs
Idle time	133 μs
Transmitted power (P_t)	14dBm

μs, with a 133 μs idle time and a 267 μs ramp time. The chirp factor, or slope, is set to 7.532 MHz/μs, giving it a bandwidth of 2GHz, resulting in 7.5 cm range resolution. The sampling frequency is selected as 5MHz, resulting in 1328 fast time samples in each T_{PRI}. A single coherent processing interval, T_{CPI}, of 0.1s duration is formed from slow time data of 250 chirps.

We have performed our experiments with two commonly used parking scenarios - the 45° angle parking and perpendicular parking as shown in Fig.1. The experimental setup for the parking test is shown in Fig.2, in which the millimeter-wave radar is situated at the origin. The dimensions of the trajectory and parking lot for conducting the parking test are selected as per the standard defined by government agencies for parking [13]. The road along the parking trajectory is 7m in width. In the angle parking case, the car must first take a straight path, and then it should be parked at 45° from the road in a parking slot that is 2.4×4.8 meters. In perpendicular parking, the car must take a straight path and then parked at 90° from the road into a parking slot that is also of the same dimensions as the previous case. For our experimental data collection, we have chosen three trajectories for each type of parking test - one correct parking trajectory and two incorrect parking trajectories. We use two small-size cars for our experiment, The first car is a Ford Figo of $3.9 \times 1.7 \times 2.5$ meters size, and the second car is a Honda Brio of a comparable size of $3.6 \times 1.7 \times 1.5$ meters.

4. RESULTS

In this section, we will first discuss the ISAR images obtained while a car is being parked in the designated parking slot. We captured measurement data for 5 seconds for each parking test. We generate 50 ISAR images for each parking test using a T_{CPI} of 0.1 seconds. In Fig 3a, we show the ISAR images for the perpendicular parking test for the Ford Figo. In each row, four images are shown corresponding to T_{CPI} equal to 3.5, 4.0, 4.5, and 5.0 s. The images from the straight-line motion of the car are not shown in these results. The first row corresponds to the ISAR images generated when the car is taking the correct trajectory and parked correctly. The second and third rows show the ISAR images for the case when the car is taking the two incorrect trajectories shown in Fig1(b) and (c); from these ISAR images, we observe the car's dimensions along with the range and cross-range. Also, in the first few view-graphs (i,ii,v and vi), we observe that the car is oriented such that the longer dimension is along with the range while the shorter is along the cross-range. Then the car undergoes a turn such that the longer dimension is along the cross-range. Along the cross-range, we also observe the micro-Doppler tracks due to the wheels of the car. In all the figures, the cross-range axis varies because this axis depends on the target's rotational velocity ω, which changes in every T_{CPI}. Our hypothesis is that based on the intensity of the ISAR image pixels corresponding to the car, we will be able to determine if the car followed the designated trajectory into the correct parking slot. Next, we show the results for the angle parking for the Ford Figo in Fig3b for the same four-time instants. Again, we show the results for the correct parking (top row), and incorrect parking due to motion along the wrong trajectories (middle and bottom rows). Then, we repeated the measurements for the Honda Brio, and show the ISAR images for perpendicular parking in Fig.4a and angle parking in Fig.4b. The top rows for both figures correspond to the case when the car executed the correct parking, while the remaining two rows show the ISAR Images when the car performs incorrect parking. Just as in the previous case, the ISAR images give information about the car's size, position and its orientation along the range and cross-range axes. In Table 2 we report the results of the parking test.We use the Ford Figo data for training and Honda Brio data for tests. The first three trajectories are for the perpendicular parking case, while the remaining three are for the angle parking. Trajectories 1 and 4 correspond to the correct parking case, while the remaining correspond to incorrect parking. Table 2 shows the normalized mean square error (NMSE) between the estimated trajectory of the test case with each of the three training cases. The results indicate that the predicted trajectory from the algorithm is matched correctly to the ground truth in all cases based on the minimum NMSE. Thus the VUT has been correctly deemed to have either passed the parking test (cases 1 and 4) or failed the test (cases 2, 3, 5 and 6).

Table 2. Result of parking test algorithm using Ford Figo data for training and Honda Brio data for test.

	Predicted Trajectory					
True Trajectory	1	2	3	4	5	6
1	**0.332**	0.387	0.347	-	-	-
2	0.361	**0.347**	0.365	-	-	-
3	0.467	0.481	**0.466**	-	-	-
4	-	-	-	**0.512**	0.534	0.615
5	-	-	-	0.558	**0.512**	0.528
6	-	-	-	0.509	0.540	**0.411**

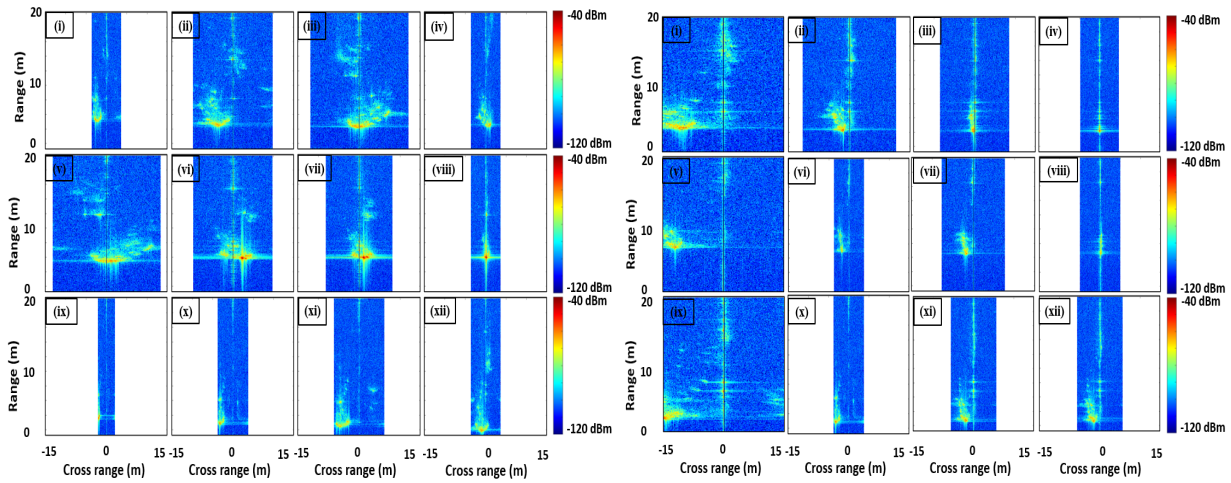

Fig. 3. ISAR images of Ford Figo carrying out (a) perpendicular parking and (b) angle parking, at 3.5, 4.0, 4.5, 5s. (1-iv) Top, (v-viii) middle, and (ix-xii) bottom rows in both images are generated for car following correct trajectory, incorrect trajectory-1, and incorrect trajectory-2 respectively.

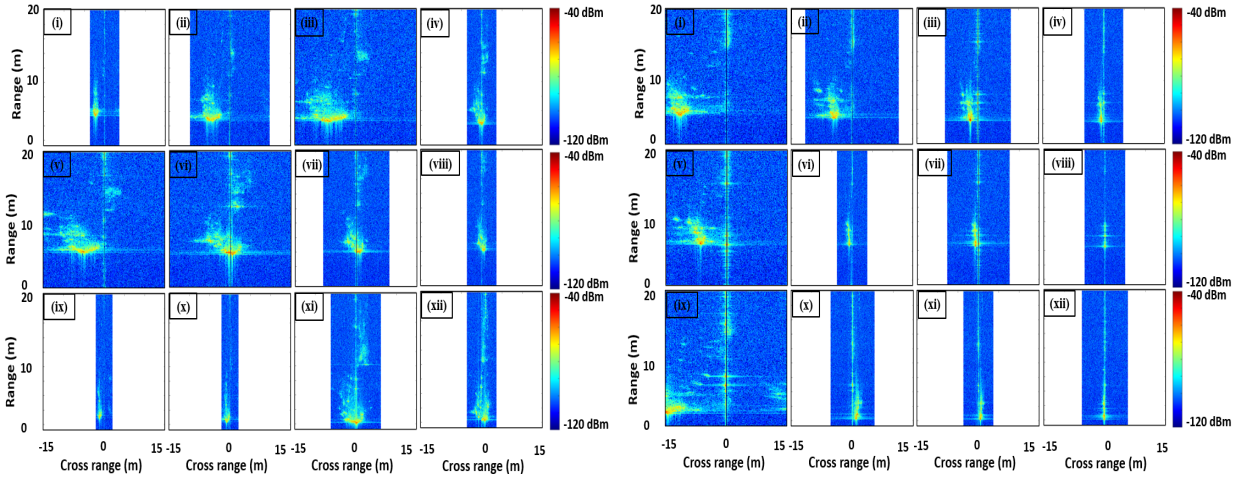

Fig. 4. Bottom row shows ISAR images of Honda Brio carrying out (a) perpendicular parking and (b) angle parking, at 3.5, 4.0, 4.5, 5s. (i-iv) Top, (v-viii) middle, and (ix-xii) bottom rows in both images are generated for car following correct trajectory, incorrect trajectory-1, and incorrect trajectory-2 respectively.

5. CONCLUSION

We have demonstrated the use of an externally mounted automotive radar to conduct automatic parking tests based on ISAR radar images. We have developed an automated parking test algorithm to classify the parking maneuvers of a VUT as either correct or incorrect based on the estimated trajectory of the VUT from the ISAR images. We have experimentally validated our proposed parking test algorithm using the data gathered using the TI-AWR 1843 millimeter-wave sensor.

6. REFERENCES

[1] A. U. Nambi, I. Mehta, A. Ghosh, V. Lingam, and V. N. Padmanabhan, "Alt: towards automating driver license testing using smartphones," in *Proceedings of the 17th Conference on Embedded Networked Sensor Systems*, 2019, pp. 29–42.

[2] J. Hasch, E. Topak, R. Schnabel, T. Zwick, R. Weigel, and C. Waldschmidt, "Millimeter-wave technology for automotive radar sensors in the 77 ghz frequency band," *IEEE Transactions on Microwave Theory and Techniques*, vol. 60, no. 3, pp. 845–860, 2012.

[3] T. Lin, H. Rivano, and F. Le Mouël, "A survey of smart parking solutions," *IEEE Transactions on Intelligent Transportation Systems*, vol. 18, no. 12, pp. 3229–3253, 2017.

[4] V. Paidi, H. Fleyeh, J. Håkansson, and R. G. Nyberg, "Smart parking sensors, technologies and applications for open parking lots: a review," *IET Intelligent Transport Systems*, vol. 12, no. 8, pp. 735–741, 2018.

[5] D. Fernández-Llorca, I. García-Daza, A. Martínez-Hellín, S. Álvarez-Pardo, and M. Á. Sotelo, "Parking assistance system for leaving perpendicular parking lots: Experiments in

daytime\nighttime conditions," *IEEE Intelligent Transportation Systems Magazine*, vol. 6, no. 2, pp. 57–68, 2014.

[6] V. C. Chen, *Inverse Synthetic Aperture Radar Imaging; Principles*. Institution of Engineering and Technology, 2014.

[7] S. Gishkori, D. Wright, L. Daniel, M. Gashinova, and B. Mulgrew, "Imaging moving targets for a forward-scanning automotive sar," *IEEE Transactions on Aerospace and Electronic Systems*, vol. 56, no. 2, pp. 1106–1119, 2019.

[8] J. S. Kulpa, M. Malanowski, D. Gromek, P. Samczynski, K. Kulpa, and A. Gromek, "Experimental results of high-resolution isar imaging of ground-moving vehicles with a stationary fmcw radar," *International Journal of Electronics and Telecommunications*, vol. 59, pp. 293–299, 2013.

[9] C. J. Li and H. Ling, "Wide-angle, ultra-wideband isar imaging of vehicles and drones," *Sensors*, vol. 18, no. 10, p. 3311, 2018.

[10] N. Pandey, G. Duggal, and S. S. Ram, "Database of simulated inverse synthetic aperture radar images for short range automotive radar," in *2020 IEEE International Radar Conference (RADAR)*. IEEE, 2020, pp. 238–243.

[11] N. Pandey and S. S. Ram, "Classification of automotive targets using inverse synthetic aperture radar images," *arXiv preprint arXiv:2101.12535*, 2021.

[12] B. Haywood and R. Evans, "Motion compensation for isar imaging," in *Proceedings of Australian Symposium on Signal processing and applications*, 1989, pp. 112–117.

[13] L. T. Authority, "Handbook on vehicle parking provision in development proposals," 2005.